Marine Pollution Bulletin 207 (2024) 116882

Contents lists available at ScienceDirect

Marine Pollution Bulletin

journal homepage: www.elsevier.com/locate/marpolbul

Plutonium in the coastal seawater around Chinese nuclear power plants: Sources, distribution, and environmental implications

Sixuan Li [a,1], Youyi Ni [b,*], Qiuju Guo [a,*]

[a] State Key Laboratory of Nuclear Physics and Technology, School of Physics, Peking University, Beijing 100871, China
[b] Institute of Nuclear Physics and Chemistry, China Academy of Engineering Physics, Mianyang 621900, China

ARTICLE INFO

Keywords:
Plutonium
Transport
Distribution coefficient
Scavenging

ABSTRACT

Coastal surface seawater samples within 30 km around ten Chinese nuclear power plants (NPPs) were systematically investigated. The $^{239+240}$Pu activity concentration in the samples varied from 0.226 mBq/m^3 to 3.098 mBq/m^3, meanwhile the ^{240}Pu/^{239}Pu atom ratios ranged from 0.151 to 0.353. Besides, the Pacific Proving Ground (PPG) close-in fallout and the global fallout were recognized as two primary sources of Pu in these samples. The $^{239+240}$Pu activity concentration as well as the PPG contribution showed similar trends as the Kuroshio intrusion path and the coastal currents in the China Seas, illustrating long-range transport and consuming of PPG derived Pu in the coastal China Seas. Moreover, accumulation of PPG sourced Pu in the Beibu Gulf were observed and was attributed to the continuous invasion of the high isotopic Pu that remobilized from the South China Sea (SCS).

1. Introduction

The anthropogenic plutonium (Pu) has been historically released into the environment since last century due to human nuclear activities including the nuclear weapon tests, nuclear power plant accidents etc. (Hu et al., 2010; Hirose and Povinec, 2015). In view of environmental radioactivity monitoring, the nuclear power plants (NPPs) are potential sources of radioactive contamination of the environment including Pu isotopes since the ^{239}Pu and ^{240}Pu are present during the operation of reactor not only via the neutron capture of ^{238}U but also due to the direct utilization of mixed oxide fuel (MOX) that contain Pu in some reactors. In recent years, China has been experiencing rapid development of nuclear energy. Until the end of 2023, there was 16 NPPs under commercial operation, with the electricity generating capacity of these NPPs counted 4.87 % of the cumulative power generation countrywide. Therefore, it is essential to investigate the current presence of Pu isotopes in the surrounding environment of these nuclear power plants to establish site-specific baseline database so that anomalous release and contamination could be correctly screened. The lessons from the Chernobyl accident and the Fukushima Daiichi Nuclear Power Plant (FDNPP) accident highlighted the necessity and importance of obtaining reliable baselines for the anthropogenic radionuclides especially long-lived radionuclides including Pu. Such close-in baselines could be informative for the sake of nuclear emergency responses and contamination assessment once nuclear accident happens. For example, based on the pre- and post-accident concentration and isotopic composition of Pu in the terrestrial and marine environment around the FDNPP, the specific source of Pu in the FDNPP reactors and the environmental impacts were evaluated by researchers (Men et al., 2019; Yamamoto et al., 2014; Zheng et al., 2013). It was observed that neither $^{239+240}$Pu concentrations nor ^{240}Pu/^{239}Pu atom ratios in the seawaters and sediments within 30 km of FDNPP exceeded the corresponding ranges before the accident, suggesting negligible influence of FDNPP derived Pu to the marine environment (Bu et al., 2014; Men et al., 2019). In China, the $^{239+240}$Pu activity concentration and ^{240}Pu/^{239}Pu atom ratio in the environment has been largely investigated in the past ten years (Li et al., 2022; Huang et al., 2022; Wu et al., 2019). Sources and spatial distribution of Pu isotopes in Chinese soils and China sea sediments have been clarified, including the surrounding soils near some NPPs (Guan et al., 2018; Ni et al., 2018a, 2020). However, compared with the cases of terrestrial soils and marine sediments, there is still lack of study on Pu in the coastal seawaters around China NPPs, which might be attributed to the difficulty of sampling and ultra-trace Pu analysis. To date, despite the crucial importance of constructing timely and representative seawater baselines

* Corresponding authors.
E-mail addresses: niyy@caep.cn (Y. Ni), qjguo@pku.edu.cn (Q. Guo).
[1] Current address: Xiaoying AI Lab, Beijing Xiaoying Technology Co., Beijing 100091, China.

https://doi.org/10.1016/j.marpolbul.2024.116882
Received 3 June 2024; Received in revised form 18 August 2024; Accepted 18 August 2024

around Chinese NPPs, data on the Pu isotopes in the coastal seawaters was still very scarce (Cao et al., 2021).

Besides, studies on the source and distribution of Pu in the seawaters are imperative to fulfill the understanding of the long-range transport and environmental behaviors of Pu in the marine environment in the China Seas. However, previous studies were mainly focused on the Pu in the sediments and the open seawaters. In contrast, investigation on Pu in the coastal seawaters in the China Seas was very limited. Recently, Wu et al. (2019) and Cao et al. (2021) summarized the current knowledge of Pu in the China Seas in the western Pacific. The riverine input and particle scavenging of Pu in the seawaters were recognized as crucial processes in the marine environment influencing the level and spatial distribution of Pu especially in the coastal areas (Cao et al., 2021; Wu et al., 2014; Zhang et al., 2022). However, these processes were mainly investigated based on the determined results of Pu in the coastal sediments. For example, Wu et al. (2014) observed higher $^{239+240}$Pu activity concentrations in the sediment on the continental shelf than the basin area and attributed it to the intense particle scavenging in the coastal shallow waters in the Pearl River Estuary. Similarly, Zhang et al. (2022) suggested that the relatively high $^{239+240}$Pu concentrations in the investigated sediments of the south China Sea (SCS) shelf were due to the scavenging and deposition of the PPG derived plutonium in that area. Because Pu has typically several-year residence time in the seawater columns, the determined Pu in the sediment samples was more like historical records while the Pu results in the seawaters were supposed to be timely. In this regard, combining the results of Pu in both seawater and sediments could be more presumable to illustrate the environmental behavior of Pu such as the particle scavenging in the coastal marine environment, and thus study on Pu in the coastal seawaters were highly required.

In this study, we systematically analyzed the coastal surface seawaters within 30 km around ten NPPs along Chinese coastline to establish site-specific and timely baseline of Pu isotopes in these areas. The sources and spatial distribution of Pu in these seawaters were investigated. On this basis, the environmental implications of these results were discussed including the transport and scavenging behaviors of Pu in the coastal China Seas.

2. Materials and methods

2.1. Sample collection

Surface seawater samples (sampling depth < 1 m) were collected around 10 nuclear power plants (NPPs) in China in 2019. The NPPs included Changjiang (CJ) NPP, Fangchengang (FCG) NPP, Yangjiang (YJ) NPP, Taishan (TS) NPP, Dayawan (DYW) NPP, Fuqing (FQ) NPP, Ningde (ND) NPP, Tianwan (TW) NPP, Haiyang (HY) NPP and Hongyanhe (HYH) NPP. The locations of each NPP were shown in Fig. 1 and the detailed sampling sites were presented in Fig. S1. The samples were collected in the vicinity of each NPP generally in a line direction with a distance of 5–30 km to the seashore. Samples were first collected into clean HDPE plastic buckets using a pumping system. Upon collection, about 100 L unfiltered seawater samples were acidified with HCl to pH 2 so as to prevent adsorption loss of Pu to the inner wall of the container. The seawater samples were shipped to local laboratories and filtered through PTFE capsule filters (0.45 μm) using a peristaltic pump before the analysis of Pu.

2.2. Analytical procedure of Pu in seawater samples

Pu isotopes in the seawater samples were analyzed using a method involving three-stage coprecipitations and two-stage anion exchange chromatography which was modified from the previous studies (Men et al., 2018; Ni et al., 2018b). Briefly, about 0.2 pg ^{242}Pu was added to the sample as a yield tracer. Then, 200 mg Fe^{3+} was added to the sample with constant stirring. Concentrated $NH_3.H_2O$ was slowly added to adjust pH to 9–11 to form $Fe(OH)_3$ precipitates. After settling for at least 4 h, the supernatant was carefully siphoned away, while the obtained Fe precipitate slurry was centrifuged at 3000 rpm for 15 min and then dissolved by 40 mL aqua regia. Dissolved sample solution was transferred into 500 mL PTFE beaker and heated at 180 °C to near dryness. About 10 mL conc. HNO_3 and 10 mL 30 % H_2O_2 were then slowly pipetted into the sample for the purpose of decomposing of organic matter in the samples. This digestion step was repeated for 2–3 times. After that, pure water was used to rinse the beaker and diluted the

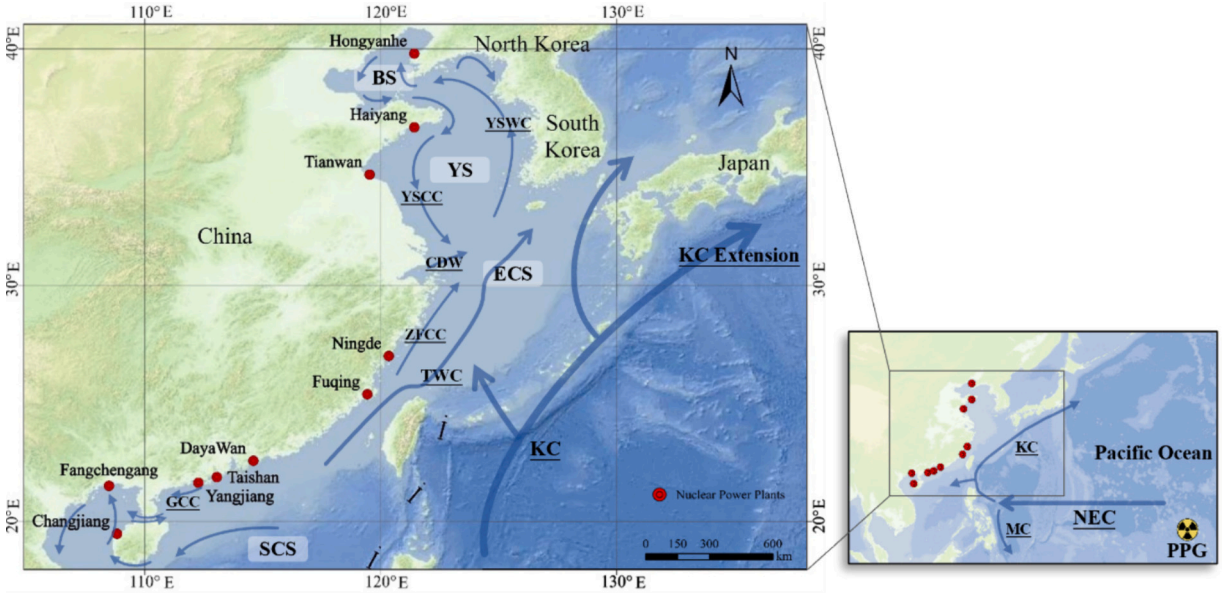

Fig. 1. Schematic Map of the locations of nuclear power plants (NPPs) and the currents in the China Seas. The red points stands for the nuclear power plants (NPPs) where our samples were collected around, and the surface currents include North Equatorial Current (NEC), Mindanao Current (MC), Kuroshio Current (KC), Beibu Gulf Current (BGC), Guangdong Coastal Current (GCC), Taiwan Warm Current (TWC), Yellow Sea Warm Current (YSWC), Yellow Sea Coastal Current (YSCC), Bohai Sea Coastal Current (BSCC), Zhejiang-Fujian Coastal Current (ZFCC), Changjiang Diluted Water (CDW). Different China seas including Bohai Sea (BS), Yellow Sea (YS), East China Sea (ECS), South China Sea (SCS) are also depicted. (For interpretation of the references to color in this figure legend, the reader is referred to the web version of this article.)

solution to about 300 mL. Again, $NH_3.H_2O$ was added to form the second stage $Fe(OH)_3$ precipitation. After removing the supernatant, the precipitate was washed with ca. 100 mL 6 M NaOH so as to further remove the amphoteric elements such as Al. The NaOH solution was also removed through centrifuging and the precipitate was dissolved with 15 mL conc. HNO_3 and then diluted with pure water to about 3 M HNO_3 condition. Next, 2 mL of 15–20 % $TiCl_3$ was added to reduce the valence of Pu to Pu(III). Subsequently, 100 mg Ca^{2+}, 100 mg La^{3+}, and 15 mL 40 % HF were successively added to the sample to conduct LaF_3/CaF_2 co-precipitation. The formed LaF_3/CaF_2 precipitate was then separated by centrifuge and dissolved with H_3BO_3 and 20 mL 3 M HNO_3. For the convenience of the subsequent anion exchange chromatography, concentrated HNO_3 was added into the sample solution to form ca. 8 M HNO_3 condition.

After the coprecipitations, a two-stage anion exchange chromatography was used for the further purification of Pu from the sample matrices. The sample solution was first loaded onto 2 mL AG 1 × 8 resin (100–200 mesh, Bio-rad Laboratories, Inc., USA) and successively rinsed with 50 mL 8 M HNO_3 and 30 mL 10 M HCl to remove U, Pb, Fe, Th, etc. Pu was then eluted from the resin with 50 mL 8.5 M HCl-0.1 M NH_4I. The eluent was heated to dryness followed by digesting with 1 mL aqua regia to remove any remaining I^-. This step was repeated twice. And then 2 mL conc. HCl was added to dissolve the residue. After adjusting the valence of Pu to Pu(IV) with 4 mL HCl/H_2O_2, the sample was loaded onto 2 mL AG MP-1M resin (100–200 mesh, Bio-rad Laboratories, Inc., USA) for further purification. The AG MP-1M resin was successively rinsed with 20 mL 8 M HNO_3 and 8 mL 10 M HCl, respectively. Finally, Pu was eluted with 16 mL HBr. After evaporating and digesting with 1 mL conc. HNO_3, the sample was dissolved in 1 mL 4 % HNO_3 for ICP-MS/MS measurement.

The Agilent 8900 ICP-MS/MS was employed for the measurement of Pu isotopes as described in our recent work (Ni et al., 2023). A novel strategy using He—O_2 collision/reaction mode was employed to improving the removal of $^{238}UH^+$ and $^{238}UH_2^+$ which were the main interferences for ^{239}Pu and ^{240}Pu detection, which contributed to the low limit of detection (LOD) of Pu isotopes. The detailed instrumental parameters were listed in Table S1 and the LOD of the analytical method were estimated to be 0.023 mBq/m^3 for ^{239}Pu and 0.037 mBq/m^3 for ^{240}Pu in 100 L seawater samples (as in Table S2).

3. Results and discussion

3.1. Spatial distribution of Pu and its scavenging in surface seawaters around NPPs

The measured concentrations and isotopic ratios of Pu in the coastal surface seawater samples around ten NPPs in China were listed in Table S3 and presented in Fig. 2 and Fig. 3. The $^{239+240}Pu$ activity concentration in the samples varied from 0.226 mBq/m^3 to 3.098 mBq/m^3, with an average of 1.267 ± 0.721 mBq/m^3 (n = 46). So far, studies on the Pu isotopes in surface seawaters of China Seas were limited, among them study regarding the coastal seawater was rather scarce probably due to the difficulty of sample collection and ultra-trace analysis of Pu. A literature summary was presented in Table 1.

The $^{239+240}Pu$ concentrations in the HYH1 and HYH2 samples which were collected in the Liaodong Bay, Bohai Sea in our study were 0.961 ± 0.047 mBq/m^3 and 0.637 ± 0.099 mBq/m^3, respectively. In the recent study of Hao et al. (2018), they revealed the levels and sources of plutonium in the surface seawaters of Liaodong Bay and Bohai Strait in China. As summarized in Table 1, a large variation of $^{239+240}Pu$ activities was reported, ranging from 1.993 to 29.677 mBq/m^3 in the Liaodong Bay (with an average of 9.471 mBq/m^3) and from 0.930 to 8.583 mBq/m^3 in the Bohai Strait (with an average of 3.534 mBq/m^3). We noticed that the surface seawater samples in the study of Hao et al. (2018) were collected at river mouths and within 10 km nearshore. The samples named HYH1 and HYH2 in our study were collected in the Liaodong Bay, which was in the same region of the Liaodong Bay samples in the study of Hao et al. (2018). However, the $^{239+240}Pu$ concentrations in the HYH1 and HYH2 were significantly lower than those in study of Hao et al. (2018). These large discrepancies were most likely deduced by the methodology differences. As described by the authors, most seawater samples in their study were turbid, illustrating the presence of large number of particles (Hao et al., 2018). However, they conducted coprecipitation and subsequent separation procedure with the seawater samples omitting prefiltration. In this context, the highly particle reactive Pu that was adsorbed by particles in the seawater should have been counted into the nominal seawater fractions, which could lead to overestimation of Pu concentration in the seawater samples. As an illustration, large variation (from 0.93 mBq/m^3 to 29.68 mBq/m^3) of $^{239+240}Pu$ activities were reported in the study and higher $^{239+240}Pu$ activities were observed at sites which were close to the riverine estuary (Hao et al., 2018).

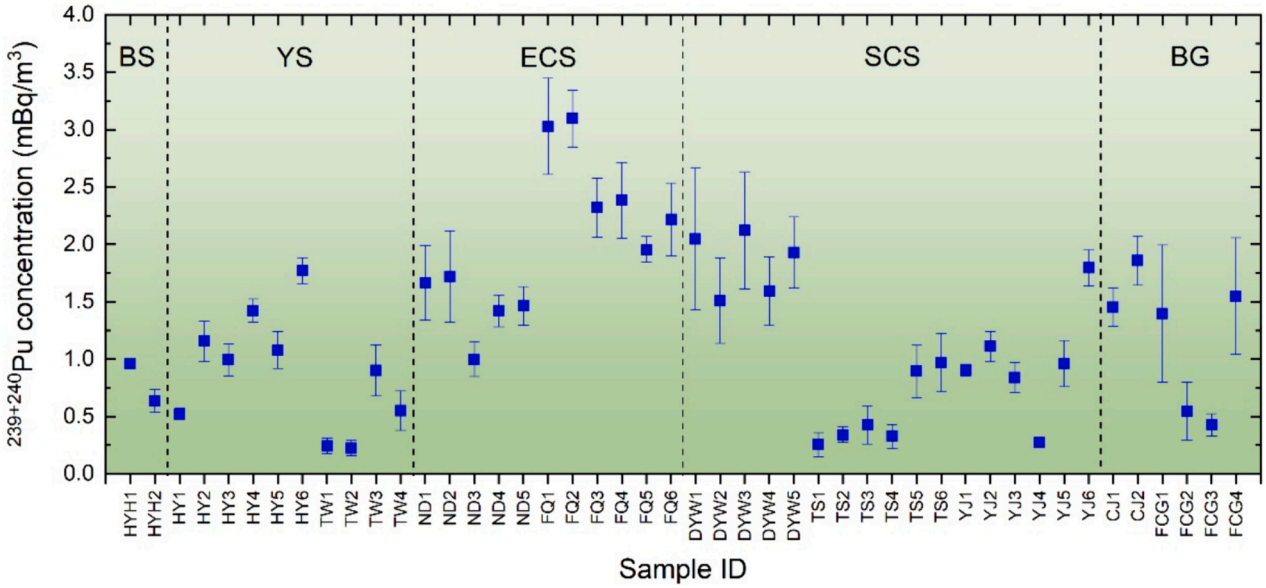

Fig. 2. $^{239+240}Pu$ activity concentration in the coastal surface seawater samples.

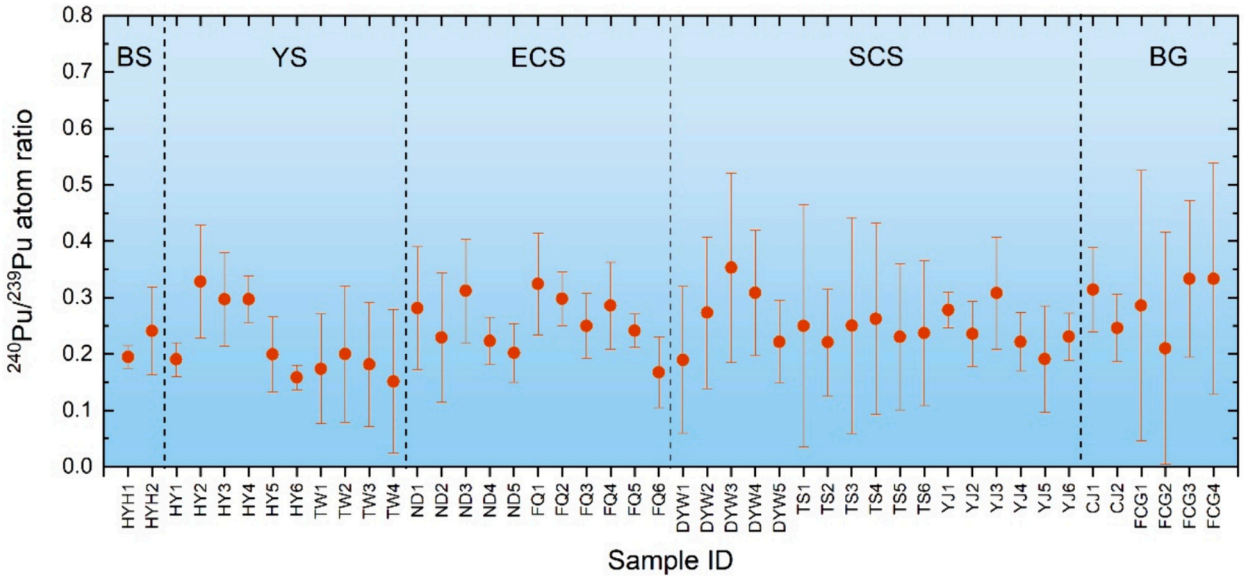

Fig. 3. ^{240}Pu/^{239}Pu atom ratio in the coastal surface seawater samples.

Table 1
Summary of $^{239+240}$Pu activity concentrations and ^{240}Pu/^{239}Pu atom ratios in surface seawater in the China Seas.

Study area	Estimated distances to the shore (km)[a]	$^{239+240}$Pu activity concentration (mBq/m^3)	^{240}Pu/^{239}Pu atom ratio	Reference
Bohai Sea (BS)	≤10 km	0.93–29.68	0.166–0.238	Hao et al., 2018
	≤30 km	0.637–0.961	0.195–0.241	This study
Yellow Sea (YS)	3–143 km	3.48–22.3	0.18–0.33	Kim et al., 2004
	111–188 km	3.2–3.7	NM[b]	Nagaya and Nakamura, 1992
	1–201 km	2.3–5.8	NM[b]	Lee et al., 2003
	≤30 km	0.226–1.772	0.151–0.328	This study
East China Sea (ECS)	≤300 km	14–24	NM[b]	Li et al., 1988
	54–189 km	5.9–84.3	NM[b]	Nagaya and Nakamura, 1992
	3–269 km	2.3–13	NM[b]	Lee et al., 2003
	NM[b]	2.8–4.2	NM[b]	Yamada and Aono, 2003
	NM[b]	NM[b]	0.199–0.246	Yamada and Zheng, 2011
	≤30 km	1.000–3.098	0.168–0.324	This study
South China Sea (SCS)	15–354 km	1.59–2.94	0.184–0.250	Wu et al., 2019
	139–305 km	2.38–2.75	0.234–0.248	Yamada and Aono, 2006
	≤417 km	2.33–7.95	NM[b]	Ahmad et al., 2010
	≤30 km	0.255–2.120	0.190–0.353	This study
Beibu Gulf	≤30 km	0.426–1.858	0.210–0.333	This study

[a] Distance either referred from the literature or estimated according to the published sampling locations and the NASA Distance to the Nearest Coastline dataset (https://oceancolor.gsfc.nasa.gov/resources/docs/distfromcoast/).
[b] NM—not mentioned.

According to Table 1, the $^{239+240}$Pu activity concentration of the coastal surface seawaters in our study was systematically lower than other seawater samples of the China seas in the referred studies. For example, Wu et al. (2018) reported the $^{239+240}$Pu activities in the SCS surface seawater ranged from 1.59 mBq/m^3 to 2.94 mBq/m^3, with an average of 2.34 ± 0.38 mBq/m^3 (n = 18). These values were much higher than the DYW (1.839 ± 0.245 mBq/m^3), TS (0.536 ± 0.286 mBq/m^3) and YJ (0.981 ± 0.448 mBq/m^3) samples in the coastal SCS. Besides, Lee et al. (2003) reported the $^{239+240}$Pu concentrations in surface water varied from 2.3 mBq/m^3 to 13 mBq/m^3 in the East China Sea, meanwhile subsurface maximum $^{239+240}$Pu concentrations up to 30 mBq/m^3 to 40 mBq/m^3 were observed at depths between 500 and 1000 m. Regarding the Yellow Sea, Kim et al. (2004) reported the $^{239+240}$Pu concentrations in the surface seawater of Yellow Sea were between 3.48 mBq/m^3 and 22.3 mBq/m^3. Therefore, it is noteworthy that the $^{239+240}$Pu concentrations in the coastal surface seawater of China seas reported in our study were distinctively lower than those in the seawater from much larger offshore distances in the aforementioned studies. We consider this difference between the coastal seawater and open seawater resulted from the enhanced particle scavenging of Pu in the coastal area.

Furthermore, two factors might lead to the enhanced particle scavenging in the coastal area. On the one hand, the particle fluxes in the coastal seawater were supposed to be larger than in the open sea. The plentiful particulate matters could be introduced to the seawater either by terrestrial riverine input or the resuspension of the sediments. Wu et al. (2014) suggested that the riverine originated particles dominated the sediment within 75 km off the Pearl River estuary in the SCS, where the DYW samples and TS samples were in the nearby region. Besides, in the coastal area the sea depth is shallow, e.g., the depths of our sampling sites were no >35 m (as shown in Table S1). Since higher hydraulic energy primarily occurs in the shallow water compared to the deep water in the offshore zone (Zhang et al., 2022), and thus under such condition the resuspension of sediment could be prevailing. An illustration of the remarkable particle flux in the coastal seawater is that some of our collected coastal surface seawater was turbid. In the marine environment, Pu has high affinity to particulate matters. Therefore, the high particle flux in the shallow coastal seawaters could lead to continuous scavenging of Pu isotopes in the seawater column into the sediment and thus resulting in lower $^{239+240}$Pu concentration in the water body. Besides, the abundant terrestrial input of nutrients and the China Coastal Current could lead to elevated biological productivity and particle fluxes (Han et al., 2012), further facilitating the scavenging of Pu from the water column on the shelf (McCubbin et al., 2004; Sholkovitz, 1983). Many previous studies have revealed the elevated inventory of $^{239+240}$Pu in the coastal sediments in different region of China seas as summarized by Wu et al. (2019) and Cao et al. (2021). For

example, in the estuary region in the ECS, the $^{239+240}$Pu inventory varied from 35.6 Bq/m^2 to 407 mBq/m^2, while BS estuary high $^{239+240}$Pu inventory of 109.9 Bq/m^2 was observed (Cao et al., 2021 and references herein). These results illustrated the accumulation of Pu in the coastal sediment was partially resulted from the scavenging of Pu in the water column, which in turn lead to the depletion of Pu in the coastal seawater.

In order to further illustrate the influence of particle scavenging on the $^{239+240}$Pu concentration in the coastal surface seawater, we roughly estimated the solid-liquid distribution coefficients (K_d) of Pu between seawater and the surface sediment in the nearby regions according to Eq. (1).

$$K_d = \frac{C_{solid}(Pu)}{C_{liquid}(Pu)} \quad (1)$$

where the C_{solid} (Pu) and C_{liquid} (Pu) represent the activity concentration of Pu in the solid phase (Bq/kg) and the liquid phase (Bq/L), respectively.

In our study, the water depth of each sampling site was <35 m, we assume that in these coastal shallow seawaters which might has high hydraulic energy the Pu in the seawater has been sufficiently mixed and was uniform in the water column. Meanwhile, we chose Pu data of the sediments that located in the nearby areas (<10 km) of our seawater sampling sites in the literature. With the $^{239+240}$Pu concentrations in our surface seawater and those in the nearby sediments, the K_d values were estimated. The $^{239+240}$Pu concentration of FCG1 seawater sample in the Beibu Gulf was 1.396 mBq/m^3. Recently, Guan et al. (2024) reported the $^{239+240}$Pu concentration in the surface sediment of Beibu Gulf, and their sampling site numbered *beibu_st.7* was only ca. 2 km from our FCG1 site. The $^{239+240}$Pu concentration of the *beibu_st.7* sample was 0.095 Bq/kg. Therefore, according to Eq. (1), the distribution coefficient of Pu at the FCG1 site was estimated to be 6.81 × 10^4 L/kg. Similarly, the site of sediment sample named *ecs_F1* in the study of Wang et al. (2017) was 8.2 km and 7.3 km away from our ND4 and ND5 sites, respectively. Thus, employing the $^{239+240}$Pu concentration in the ND4 seawater, ND5 seawater and the *ecs_F1* sediment, we estimated the K_d of Pu at the ND4 and ND5 were 1.54 × 10^5 L/kg and 1.50 × 10^5 L/kg, respectively. McDonald et al. (2001) determined the K_d of Pu in the seawater-sediment system by re-dissolution Irish sediment with Irish seawater after 1-week stirring. The measured K_d were 0.50 × 10^5 L/kg to 2.07 × 10^5 L/kg with an average of 1.20 × 10^5 L/kg. Besides, Lin et al. (2006) reported the K_d of Pu was 1.22 × 10^5 L/kg by measuring the $^{239+240}$Pu in the seawater and sediment in the coastal sea of Korea. In summary, our estimated K_d values of Pu in the coastal China sea were comparable to those reported in the Irish sea and the coastal sea of Korea. According to the IAEA (2010), the K_d of Pu in the freshwater ecosystems has a wide range between 1.1 × 10^4 L/kg and 5.2 × 10^6 L/kg. It could be concluded that the estimated K_d of Pu in our study and the studies of McDonald et al. (2001) and Lin et al. (2006) were much more concentrate. Therefore, we considered the high K_d of Pu was contributive for the enhanced particle scavenging of Pu in the coastal seawaters and consequently lead to the relatively low concentration of $^{239+240}$Pu in the coastal seawater.

The spatial variation of $^{239+240}$Pu activity concentration in the surface samples around different NPPs in different latitude was depicted in Fig. 2 and summarized in Table 2. The highest mean $^{239+240}$Pu activity was observed near the FQ NPP (2.500 ± 0.420 mBq/m^3), and followed by the DYW NPP (1.839 ± 0.245 mBq/m^3). The $^{239+240}$Pu activity concentration showed a decreasing trend northward from the FQ NPP. Specifically, the $^{239+240}$Pu activity concentrations decrease in the order of FQ > ND > HY > HYH, which was inverse of their latitudes. The samples collected around TW NPP had the lowest $^{239+240}$Pu activity concentration among all the NPPs. This phenomenon was most likely attributed to the geographical condition of the sampling locations. The TW samples were collected in the coastal region of Lianyungang city, near the Port of Lianyungang, which is the largest port in Jiangsu province. Since large-tonnage cargo ships frequently enter and leave the port, it might cause more intense turnover of the sediment and consequently facilitate the particle scavenging of Pu from the water column, and finally resulted in the relatively low $^{239+240}$Pu concentrations in these seawater samples. Meanwhile, the $^{239+240}$Pu activity concentrations showed a southward decreasing trend in the order of DYW > YJ > FCG, which was the same as the order of their latitudes. The variations of the $^{239+240}$Pu activity concentration in the seawater northwards from the FQ NPP and southwards from the DYW NPP were both primarily related to the long-range transport of Pu, which would be discussed in the next section.

Table 2
Contributions of PPG in different nearshore regions around nuclear power plant bases.

Nearby nuclear power plants (NPPs)	Mean $^{239+240}$Pu concentration (mBq/m^3)	Mean ^{240}Pu/^{239}Pu atom ratio	Mean fraction of PPG
Changjiang (CJ)	1.655 ± 0.203	0.280 ± 0.034	63 %
Fangchengang (FCG)	0.980 ± 0.498	0.291 ± 0.050	67 %
Yangjiang (YJ)	0.981 ± 0.448	0.244 ± 0.038	42 %
Taishan (TS)	0.536 ± 0.286	0.242 ± 0.014	42 %
Dayawan (DYW)	1.839 ± 0.245	0.269 ± 0.059	54 %
Fuqing (FQ)	2.500 ± 0.420	0.261 ± 0.050	52 %
Ningde (ND)	1.453 ± 0.254	0.250 ± 0.041	45 %
Tianwan (TW)	0.480 ± 0.275	0.177 ± 0.017	4 %
Haiyang (HY)	1.158 ± 0.384	0.245 ± 0.064	42 %
Hongyanhe (HYH)	0.799 ± 0.162	0.218 ± 0.023	26 %

3.2. Source term and transport of Pu in the coastal seawaters in China Seas

As presented in Table 2, the ^{240}Pu/^{239}Pu atom ratio in the investigated seawater samples varied from 0.151 to 0.353, meanwhile the overall average was 0.248 ± 0.052 (n = 46). In general, the ^{240}Pu/^{239}Pu atom ratios in these coastal seawaters were comparable with the reported ^{240}Pu/^{239}Pu atom ratios in seawaters in the SCS (0.184–0.250) (Wu et al., 2019; Yamada and Aono, 2006), the ECS (0.199–0.246) (Yamada and Zheng, 2011) the YS (0.18–0.33) (Kim et al., 2004) and the BS (0.166–0.238) (Hao et al., 2018), respectively. Nevertheless, the ^{240}Pu/^{239}Pu atom ratios in the FCG and CJ samples (both located in the Beibu Gulf) were apparently higher than the aforementioned values in China Seas; meanwhile the ^{240}Pu/^{239}Pu atom ratio in the TW samples were lower than the reported values.

These characteristic ^{240}Pu/^{239}Pu atom ratios were remarkably different from the typical global fallout value 0.176–0.186 (Kelley et al., 1999; Krey et al., 1976; Li et al., 2022; Xu et al., 2018), illustrating other sources besides the global fallout. In the 1950s, a series of nuclear tests was conducted by United States in the Pacific Proving Grounds (PPG), which were characterized by high ^{240}Pu/^{239}Pu atom ratios (0.30–0.36) (Buesseler, 1997; Diamond et al., 1960; Koide et al., 1985; Muramatsu et al., 2001). Until 2015, the $^{239+240}$Pu activity concentrations in seawaters of lagoons in the PPG were still >400 mBq/m^3, and thus the PPG remained as a net source of Pu to the North Pacific (Buesseler et al., 2018). As a result, it was estimated that an annual $^{239+240}$Pu export flux of 0.3–0.7 TBq released into the North Pacific Ocean from the PPG (Buesseler et al., 2018). In the recent study of Men et al. (2018), high contribution of PPG up to 84 % has been found in the Northwest Pacific seawaters. The Fukushima Daiichi Nuclear Power Plant (FDNPP) accident had similarly high ^{240}Pu/^{239}Pu atom ratio (0.330 ± 0.032) to the PPG-derived Pu (Zheng et al., 2013). However, based on the studies on the $^{239+240}$Pu activity and ^{240}Pu/^{239}Pu atom ratio in both sediments and seawaters around the FDNPP, no significant difference was found before and after the accident, suggesting the influence of FDNPP sourced Pu on the west North Pacific was negligible (Bu et al., 2014; Men et al., 2018;

Oikawa et al., 2015; Zheng et al., 2013). Furthermore, reports on the $^{241}Pu/^{239}Pu$ ratio and ^{241}Pu concentration in seawater along the Japanese coast and eastern North Pacific further confirmed that the FDNPP accident had little effects to the marine environment (Hain et al., 2017). For these reasons, the global fallout and the PPG were supposed to be the two sources of Pu in the investigated seawater samples. By employing the two end-member mixing model, the respective contributions of the PPG and the global fallout in these seawaters could be evaluated as Eq. (2) and Eq. (3).

$$\frac{\mathrm{Pu(PPG)}}{\mathrm{Pu(Global)}} = \frac{(R_G - R_S)(1 + 3.674R_P)}{(R_S - R_P)(1 + 3.674R_G)} \quad (2)$$

$$\mathrm{Pu(PPG)} + \mathrm{Pu(Global)} = 100\ \% \quad (3)$$

where R represents the $^{240}Pu/^{239}Pu$ atom ratio. The subscripts P, G and S refer to the PPG, global fallout, and the investigated samples, respectively. The coefficient 3.674 was used for conversion between activity ratios and the atom ratios of $^{240}Pu/^{239}Pu$. The values of R_G and R_P were 0.176 (Krey et al., 1976) and 0.36 (Buesseler, 1997), respectively.

The mean $^{240}Pu/^{239}Pu$ atom ratios together with the corresponding contribution of PPG in the coastal seawaters around different NPPs were shown in Table 2. The spatial variation of the $^{240}Pu/^{239}Pu$ showed the similar trends as the aforementioned $^{239+240}Pu$ activity concentration, which was influenced by the transport of Pu. Specifically, the FQ (0.261 ± 0.050) and DYW (0.269 ± 0.059) NPPs had relatively high $^{240}Pu/^{239}Pu$ atom ratios. On the one hand, with the increasing of latitude, the $^{240}Pu/^{239}Pu$ atom ratio decreased in the order of FQ > ND > HY > HYH, and implied the decreasing contribution of the PPG close-in fallout. In the FQ samples the contribution of PPG were approximately 52 %, while around the northernmost HYH NPP the PPG derived Pu only counted for 26 % of the total Pu in the surface seawaters; on the other hand, with the decreasing of latitude from the DYW NPP to the YJ NPP, a decreasing trend of $^{240}Pu/^{239}Pu$ atom ratio was also observed. Correspondingly, the contribution of PPG derived Pu in the surface seawaters decreased from 54 % around the DYW NPP to 42 % around the YJ NPP. The spatial variations of $^{239+240}Pu$ concentration and the $^{240}Pu/^{239}Pu$ atom ratio were supposed to be a result of multiple factors such as the geographical and hydrological conditions, the transport and remobilization of the PPG close-in fallout in the North Pacific etc. Fig. 1 roughly marked the currents and potential transport paths of the PPG close-in Pu in the western North Pacific. Pu isotopes released from the contaminated lagoons at the PPG sites in the central North Pacific were continuously conveyed by the North Equatorial Current westward the Philippine Sea. The North Equatorial Current splits into the northward-flowing Kuroshio Current which partially extends into the northern South China Sea through the Luzon Strait while the main stream travels northeast along the boundary of China Seas (Wang et al., 2017; Wu et al., 2019). The FQ NPP and DYW NPP were located near the northward bifurcation of the Kuroshio branch which flows into the SCS. In the northward direction, the Taiwan Warm Current brings the PPG derived Pu along the coastal areas to the ECS, which passes the area of ND NPP. Meanwhile, the main stream of Kuroshio flows northeastward along the eastern coast of Taiwan and a branch of the Kuroshio enters the Taiwan Current (TWC) in the ECS at the northeast corner of Taiwan (Ichikawa and Beardsley, 2002). In the tail of the TWC, the Yellow Sea Warm Current conveys the PPG-Pu anticlockwise in the Yellow Sea and reached the area of HY NPP with the Yellow Sea Coastal Current (YSCC), while a branch of the YSWC split into the Bohai Strait where our HYH samples were collected. The Pu from PPG were continuously consumed by mixing with the global fallout Pu in the seawater along the aforementioned paths, and thus resulted in decreasing trend of the PPG contribution. Similarly, in the SCS, a branch of the Kuroshio brings the PPG sourced Pu counterclockwise from the north shelf to the south basin of the SCS with a part of the current invades into the Beibu Gulf from the southern mouth of the Beibu Gulf. Besides, in the coastal areas in the SCS, the Guangdong Coastal Current (GCC) flows from Guangdong province southwestward along the coast to the Beibu Gulf through the Qiongzhou Strait, which passed by the DYW, TS, and YJ NPPs, subsequently. Along the route of currents in these coastal areas, Pu in the seawaters were largely removed from the water body due to high scavenging efficiency in the coastal seawaters. In this way, the contribution of PPG sourced Pu in the surface seawaters around these NPPs decreased in the southwest direction. Therefore, our results proved that the contribution of Pu in the coastal seawaters in China Seas agrees with the route of the surface currents.

A noteworthy phenomenon is that the mean $^{240}Pu/^{239}Pu$ atom ratio in the FCG and CJ samples were relatively high, reaching 0.291 ± 0.050 and 0.280 ± 0.034, respectively. Accordingly, the contributions of PPG derived Pu in the FCG and CJ samples were >60 % and were higher than those in other coastal seawater samples investigated in this study. Besides, the $^{240}Pu/^{239}Pu$ atom ratio in FCG and CJ samples were also apparently higher than those in the surface seawaters in the SCS reported by Wu et al. (2018) where the ratios were 0.184 to 0.250 with an average of 0.231 ± 0.018 (n = 18). Our results were also higher than the previously reported $^{240}Pu/^{239}Pu$ values (0.242 ± 0.007, n = 3) in the SCS basin (Yamada and Aono, 2006). Furthermore, the recent studies of Guan et al. (2021, 2024) revealed the average $^{240}Pu/^{239}Pu$ atom ratios in the sediments and corals in the Beibu Gulf were 0.236 and 0.203, respectively. It could be concluded that the $^{240}Pu/^{239}Pu$ atom ratios in the seawaters in the Beibu Gulf were apparently higher than in the outer SCS seawaters as well as the sediments and corals in the Beibu Gulf. Nevertheless, the $^{239+240}Pu$ activity concentration in the FCG (0.980 ± 0.498 mBq/m^3) and CJ (1.655 ± 0.203 mBq/m^3) samples were still lower than the $^{239+240}Pu$ activities which were 1.59 mBq/m^3–7.95 mBq/m^3 in the outer SCS surface seawaters (Ahmad et al., 2010; Wu et al., 2019; Yamada and Aono, 2006). These results might imply the accumulation of PPG derived Pu in the seawater of Beibu Gulf. The following reasons were possible for such phenomenon. 1) In the northern shore of Beibu Gulf where the FCG samples collected there were few rivers flowing into the sea, and the primary source of sediment originated from Guangdong Province through the Qiongzhou Strait (Xu et al., 2022). Therefore, the fraction of Pu from the land-origin was relatively smaller compared to other coastal areas such as the sampling sites of DYW, TS and YJ samples near the Pearl River Estuary where the riverine originated particles dominate the sediment within 75 km off the estuary (Wu et al., 2014). For the CJ samples, although the sampling sites were near the Changhua River, the influence of riverine input of Pu in the samples might be not significant as the $^{239+240}Pu$ activity concentration in the soils in Hainan were extremely low (0.043–0.073 Bq/kg) according to Zhang et al. (2022). 2) As depicted in Fig. 1, the water mass flows into the Beibu Gulf from the SCS both through the Qiongzhou Strait and from the southern bay mouth of the Beibu Gulf. Therefore, the SCS acted as a transitional reservoir of Pu from the PPG and meanwhile a secondary source for the Beibu Gulf. In the previous studies of Wu et al. (2019), the accumulation of non-global fallout Pu in the SCS were found where higher $^{239+240}Pu$ activity and PPG contribution in the SCS were recognized compared to the adjacent ECS. Besides, enhanced transformation/deposition of plutonium through biogeochemical process in the continental shelf and deep ocean of SCS were possible as suggested by Zhang et al. (2022). Therefore, we consider that the high $^{240}Pu/^{239}Pu$ ratio in the Beibu Gulf might be associated with the continuous invasion of the high isotopic Pu that accumulated and remobilized from the SCS.

4. Conclusions and perspectives

In this study, coastal surface seawater samples within 30 km around ten Chinese nuclear power plants were collected. The Pu isotopes in these seawater samples were analyzed to establish site-specific and timely baseline around these NPPs. The $^{239+240}Pu$ activity concentration in the samples varied from 0.226 mBq/m^3 to 3.098 mBq/m^3, meanwhile the $^{240}Pu/^{239}Pu$ atom ratios ranged from 0.151 to 0.353. The $^{239+240}Pu$ activity concentration in these coastal seawaters were substantially

lower than the reported values in the open seas, which might be due to enhanced particle scavenging in the coastal areas. By applying the characteristic $^{240}Pu/^{239}Pu$ atom ratio as fingerprinting clue, the global fallout and the PPG close-in fallout were considered as the sources of Pu in these samples. Regarding the spatial distribution of Pu, the highest mean $^{239+240}Pu$ activity was observed near the FQ NPP and DYW NPP in the SCS, which were 2.500 ± 0.420 mBq/m^3 (n = 6) and 1.839 ± 0.245 mBq/m^3 (n = 5), respectively. Then, the $^{239+240}Pu$ activity concentration showed decreasing trends northward from the FQ NPP and southward from the DYW NPP. This was in agreement with the Kuroshio intrusion path and the coastal currents in the China Seas, which could be evidence for the long-range transport and consuming of PPG derived Pu in the coastal areas in the China Sea. Besides, high $^{240}Pu/^{239}Pu$ atom ratios near the FCG and CJ NPPs in the Beibu Gulf were observed, where >60 % of Pu were contributed from the PPG. The accumulation of PPG sourced Pu in the Beibu Gulf was attributed to the small land-origin input of global fallout Pu and the continuous invasion of the high isotopic Pu that accumulated and remobilized from the SCS. In contrast, the lowest $^{239+240}Pu$ concentrations (0.480 ± 0.275 mBq/m^3) as well as $^{240}Pu/^{239}Pu$ atom ratios (0.177 ± 0.017) were determined around the TW NPP, which was likely caused by the intense turnover of sediments and scavenging of particles in the seawater since the sampling sites were close to a port. Finally, we estimated the distribution coefficients of Pu in the coastal areas in the China Seas using our determined Pu data of the seawater and those of the nearby coastal sediments from the literature. The estimated distribution coefficients (K_d) of Pu varied from 6.81 × 10^4 L/kg to 1.54 × 10^5 L/kg. For the future study, more accurate determination of the K_d in the coastal area is required via concurrent analysis of both the seawater and suspended particles. The K_d of Pu could be useful to estimate $^{239+240}Pu$ concentration in the shallow nearshore seawater in areas where the $^{239+240}Pu$ concentration in sediments were available. This would be convenient since the Pu analysis in sediments was more efficient and simpler than that in seawater samples.

CRediT authorship contribution statement

Sixuan Li: Writing – original draft, Methodology, Investigation, Formal analysis, Data curation. **Youyi Ni:** Writing – review & editing, Visualization, Validation, Investigation, Funding acquisition, Formal analysis, Conceptualization. **Qiuju Guo:** Visualization, Validation, Supervision, Resources, Project administration, Funding acquisition, Conceptualization.

Declaration of competing interest

None.

Data availability

Data will be made available on request.

Acknowledgements

This work was supported by the National Natural Science Foundation of China (Grant Numbers 12305355 and 12075009).

Appendix A. Supplementary data

Supplementary data to this article can be found online at https://doi.org/10.1016/j.marpolbul.2024.116882.

References

Ahmad, Z., Mei-Wo, Y., Abu Bakar, A.S., Shahar, H., 2010. Spatial distributions of ^{137}Cs and $^{239+240}Pu$ in surface seawater within the Exclusive Economic Zone of East Coast Peninsular Malaysia. Appl. Radiat. Isot. 68 (9), 1839–1845.

Bu, W.T., Fukuda, M., Zheng, J., Aono, T., Ishimaru, T., Kanda, J., Yang, G.S., Tagami, K., Uchida, S., Guo, Q.J., Yamada, M., 2014. Release of Pu isotopes from the Fukushima Daiichi nuclear power plant accident to the marine environment was negligible. Environ. Sci. Technol. 48 (16), 9070–9078.

Buesseler, K., 1997. The isotopic signature of fallout plutonium in the North Pacific. J. Environ. Radioact. 36, 69–83.

Buesseler, K., Charette, M., Pike, S., Henderson, P., Kipp, L.E., 2018. Lingering radioactivity at the Bikini and Enewetak atolls. Sci. Total Environ. 621, 1185–1198.

Cao, L.G., Zheng, J., Zhou, Z.C., Bu, W.T., Wang, Z.T., Zheng, W., Yamada, M., 2021. Distribution and behavior of plutonium isotopes in Western Pacific marginal seas. Catena 198, 105023.

Diamond, H., Fields, P.R., Stevens, C.S., Studier, M.H., Fried, S.M., Inghram, M.G., Hess, D.C., Pyle, G.L., Mech, J.F., Manning, W.M., Ghiorso, A., Thompson, S.G., Higgins, G.H., Seaborg, G.T., Browne, C.I., Smith, H.L., Spence, R.W., 1960. Heavy isotope abundances in "Mike" thermonuclear device. Phys. Rev. 119, 2000–2004.

Guan, Y.J., Sun, S.Y., Sun, S.M., Wang, H.J., Ruan, X.D., Liu, Z.Y., Terrasi, F., Gialanella, L., Shen, H.T., 2018. Distribution and sources of plutonium along the coast of Guangxi, China. Nucl. Instrum. Methods Phys. Res. B 437, 61–65.

Guan, Y.J., Mai, J.Y., Wang, H.J., Zhang, P.J., Huang, C.P., Liu, Z.Y., Zhan, X.Y., Cesare, M.D., He, X.W., Wang, X.G., Ye, M., 2021. Plutonium isotopes and radionuclides in corals around Weizhou land in Beibu Gulf, China. Appl. Radiat. Isot. 176, 109873.

Guan, Y.J., He, H., Fan, K.D., Wang, S.Z., Guo, Z.C., Wang, H.J., Cui, L.J., Chen, W., Huang, C.P., Liu, Z.Y., He, X.W., Guo, K.X., Zhang, J.J., Xu, Z.Y., 2024. Spatial distribution, source identification, and transportation paths of plutonium in the Beibu Gulf, South China Sea. Mar. Pollut. Bull. 199, 115972.

Hain, K., Faestermann, T., Fimiani, L., Golser, R., Gómez-Guzmán, J.M., Korschinek, G., Kortmann, F., Von Gostomski, C.L., Ludwig, P., Steier, P., Tazoe, H., Yamada, M., 2017. Plutonium isotopes ($^{239-241}Pu$) dissolved in Pacific Ocean waters detected by Accelerator Mass Spectrometry: no effects of the Fukushima Accident observed. Environ. Sci. Technol. 51 (4), 2031–2037.

Han, A.Q., Dai, M.H., Kao, S.J., Gan, J.P., Li, Q., Wang, L.F., Zhai, W.D., Wang, L., 2012. Nutrient dynamics and biological consumption in a large continental shelf system under the influence of both a river plume and coastal upwelling. Limnol. Oceanogr. 57, 486–502.

Hao, Y.P., Pan, S.M., Song, X.W., Zhang, K.X., Guo, H.T., Gu, Z., 2018. Sources of plutonium isotopes and ^{137}Cs in coastal seawaters of Liaodong Bay and Bohai Strait, China and its environmental implications. Mar. Pollut. Bull. 130, 240–248.

Hirose, K., Povinec, P., 2015. Sources of plutonium in the atmosphere and stratosphere-troposphere mixing. Sci. Rep. 5, 15707.

Hu, Q.H., Weng, J.Q., Wang, J.S., 2010. Sources of anthropogenic radionuclides in the environment: a review. J. Environ. Radioact. 101, 426–437.

Huang, Y.N., Sun, X.M., Zhang, W., Xiao, Z., 2022. Spatial distribution and migration of $^{239+240}Pu$ in Chinese soils. Sci. Total Environ. 824, 153724.

IAEA (International Atomic Energy Agency), 2010. Handbook of Parameter Values for the Prediction of Radionuclide Transfer in Terrestrial and Freshwater Environments.

Ichikawa, H., Beardsley, R.C., 2002. The current system in the Yellow and East China Seas. J. Oceanogr. 58, 77–92.

Kelley, J.M., Bond, L.A., Beasley, T.M., 1999. Global distribution of Pu isotopes and ^{237}Np. Sci. Total Environ. 237–238, 483–500.

Kim, C.K., Kim, C.S., Chang, B.U., Choi, S.W., Chung, C.S., Hong, G.H., Hirose, K., Igarashi, Y., 2004. Plutonium isotopes in seas around the Korean Peninsula. Sci. Total Environ. 318 (1–3), 197–209.

Koide, M., Bertine, K.K., Chow, T.J., Goldberg, E.D., 1985. The $^{240}Pu/^{239}Pu$ ratio, a potential geochronometer. Earth Planet. Sci. Lett. 72 (1), 1–8.

Krey, P.W., Hardy, E.P., Pachucki, C., Rourke, F., Coluzza, J., Benson, W.K., 1976. Mass isotopic composition of global fallout plutonium in soil. In: Transuranium Nuclides in the Environment (Proceedings Series). IAEA, Vienna, pp. 671–678.

Lee, S.H., Gastaud, J., Povinec, P.P., Hong, G.H., Kim, S.H., Chung, C.S., Lee, K.W., Pettersson, H.B.L., 2003. Distribution of plutonium and americium in the marginal seas of the northwest Pacific Ocean. Deep-Sea Res. Pt. II 50 (17), 2727–2750.

Li, P.Q., Yan, Q.M., Yu, Y.T., 1988. The determination of plutonium in surface seawater of Okinawa trough and East China Sea. Mar. Sci. 3, 43–46 (in Chinese).

Li, S.X., Ni, Y.Y., Guo, Q.J., 2022. Sources and variability of plutonium in Chinese soils: a statistical perspective with moving average. Atmosphere 13 (5), 769.

Lin, X., Park, G., Kwak, J., Kim, W., Kang, H., Lee, H., Kim, Y., Doh, S., Kim, D., Kim, C., 2006. $^{239+240}Pu$ concentrations of sediments and seawater in the coastal sea of Korea. J. Radioanal. Nucl. Chem. 268, 103–108.

McCubbin, D., Leonard, K.S., Greenwood, R.C., Taylor, B.R., 2004. Solid-solution partitioning of plutonium in surface waters at the Atomic Weapons Establishment Aldermaston (UK). Sci. Total Environ. 332, 203–216.

McDonald, P., Batlle, J., Bousher, A., Whittall, A., Chambers, N., 2001. The availability of plutonium and americium in Irish Sea sediments for re-dissolution. Sci. Total Environ. 267, 109–123.

Men, W., Zheng, J., Wang, H., Ni, Y.Y., Aono, T., Maxwell, S.L., Tagami, K., Uchida, S., Yamada, M., 2018. Establishing rapid analysis of Pu isotopes in seawater to study the impact of Fukushima nuclear accident in the Northwest Pacific. Sci. Rep. 8, 1892.

Men, W., Zheng, J., Wang, H., Ni, Y.Y., Kumamoto, Y., Yamada, M., Uchida, S., 2019. Pu isotopes in the seawater off Fukushima Daiichi Nuclear Power Plant site within two months after the severe nuclear accident. Environ. Pollut. 246, 303–310.

Muramatsu, Y., Hamiton, T., Uchida, S., Tagami, K., Yoshida, S., Robison, W., 2001. Measurement of $^{240}Pu/^{239}Pu$ isotopic ratios in soils from the Marshall Islands using ICP-MS. Sci. Total Environ. 278, 151–159.

Nagaya, Y., Nakamura, K., 1992. $^{239,240}Pu$ and ^{137}Cs in the East China and the Yellow Seas. J. Oceanogr. 48 (1), 23–35.

Ni, Y.Y., Wang, Z.T., Guo, Q.J., Zheng, J., Li, S.X., Lin, J.X., Tan, Z.Y., Huang, W.N., 2018a. Distinctive distributions and migrations of $^{239+240}$Pu and ^{241}Am in Chinese forest, grassland and desert soils. Chemosphere 212, 1002–1009.

Ni, Y.Y., Zheng, J., Guo, Q.J., Wang, H., Tagami, K., Uchida, S., 2018b. Comparisons of soil pretreatment methods for SF-ICP-MS determination of ultra-trace level plutonium in water soluble and exchangeable fractions. J. Radioanal. Nucl. Chem. 315, 643–651.

Ni, Y.Y., Guo, G.J., Huang, Z.Y., Zheng, J., Li, S.X., Huang, W.N., Bu, W.T., 2020. First study of ^{237}Np in Chinese soils: source, distribution and mobility in comparison with plutonium isotopes. Chemosphere 252, 126683.

Ni, Y.Y., Bu, W.T., Xiong, K., Hu, S., Yang, C.T., Cao, L.G., 2023. A novel strategy for Pu determination in water samples by automated separation in combination with direct ICP-MS/MS measurement. Talanta 262, 124710.

Oikawa, S., Watabe, T., Takata, H., 2015. Distributions of Pu isotopes in seawater and bottom sediments in the coast of the Japanese archipelago before and soon after the Fukushima Daiichi Nuclear Power Station accident. J. Environ. Radioact. 142, 113–123.

Sholkovitz, E.R., 1983. The geochemistry of plutonium in fresh and marine water environments. Earth Sci. Rev. 19, 95–161.

Wang, J.L., Baskaran, M., Hou, X.L., Du, J.Z., Zhang, J., 2017. Historical changes in ^{239}Pu and ^{240}Pu sources in sedimentary records in the East China Sea: implications for provenance and transportation. Earth Planet. Sci. Lett. 466, 32–42.

Wu, J.W., Zheng, J., Dai, M.H., Huh, C.A., Chen, W.F., Tagami, K., Uchida, S., 2014. Isotopic composition and distribution of plutonium in northern South China Sea sediments revealed continuous release and transport of Pu from the Marshall Islands. Environ. Sci. Technol. 48, 3136–3144.

Wu, J.W., Sun, J., Xiao, X.Y., 2019. An overview of current knowledge concerning the inventory and sources of plutonium in the China Seas. Mar. Pollut. Bull. 150, 110599.

Xu, D., Ge, Q., Han, X.B., Deng, T., Xiao, T.L., 2022. Driving force of marine sedimentary source to sink: a case study from Beibu Gulf. J. Mar. Sci. 40, 17–32.

Xu, Y.H., Pan, S.M., Gao, J.H., Hou, X.L., Ma, Y.F., Hao, Y.P., 2018. Sedimentary record of plutonium in the North Yellow Sea and the response to catchment environmental changes of inflow rivers. Chemosphere 207, 130–138.

Yamada, M., Aono, T., 2003. Vertical profiles of $^{239+240}$Pu in seawater from the East China Sea. J. Radioanal. Nucl. Chem. 256 (3), 399–402.

Yamada, M., Aono, T., 2006. ^{238}U, Th isotopes, ^{210}Pb and $^{239+240}$Pu in settling particles on the continental margin of the East China Sea: fluxes and particle transport processes. Mar. Geol. 227, 1–12.

Yamada, M., Zheng, J., 2011. Determination of ^{240}Pu/^{239}Pu atom ratio in seawaters from the East China Sea. Radiat. Prot. Dosimetry 146 (1–3), 311–313.

Yamamoto, M., Sakaguchi, A., Ochiai, S., Takada, T., Hamataka, K., Murakami, T., Nagao, S., 2014. Isotopic Pu, Am and Cm signatures in environmental samples contaminated by the Fukushima Daiichi Nuclear Power Plant accident. J. Environ. Radioact. 132, 31–46.

Zhang, M.T., Qiao, J.X., Zhang, W.C., Zhu, L.C., Hou, X.L., 2022. Plutonium isotopes in the northwestern South China Sea: level, distribution, source and deposition. Environ. Pollut. 298, 118846.

Zheng, J., Tagami, K., Uchida, S., 2013. Release of plutonium isotopes into the environment from the Fukushima Daiichi Nuclear Power Plant Accident: what is known and what needs to be known. Environ. Sci. Technol. 47, 9584–9595.